AEM
Journals.ASM.org

Vernalophrys algivore gen. nov., sp. nov. (Rhizaria: Cercozoa: Vampyrellida), a New Algal Predator Isolated from Outdoor Mass Culture of *Scenedesmus dimorphus*

Yingchun Gong,[a,b,c] David J. Patterson,[d] Yunguang Li,[e] Zixuan Hu,[f] Milton Sommerfeld,[c] Yongsheng Chen,[f] Qiang Hu[a,b,c]

Center for Microalgal Biotechnology and Biofuels, Institute of Hydrobiology, Chinese Academy of Sciences, Wuhan, China[a]; Key Laboratory for Algal Biology, Institute of Hydrobiology, Chinese Academy of Sciences, Wuhan, China[b]; Laboratory for Algae Research and Biotechnology, College of Technology and Innovation, Arizona State University, Mesa, Arizona, USA[c]; School of Biological Sciences, University of Sydney, Sydney, New South Wales, Australia[d]; College of Life Sciences and Technology, Huazhong Agricultural University, Wuhan, China[e]; School of Civil and Environmental Engineering, Georgia Institute of Technology, Atlanta, Georgia, USA[f]

Microbial contamination is the main cause of loss of biomass yield in microalgal cultures, especially under outdoor environmental conditions. Little is known about the identities of microbial contaminants in outdoor mass algal cultures. In this study, a new genus and species of vampyrellid amoeba, *Vernalophrys algivore*, is described from cultures of *Scenedesmus dimorphus* in open raceway ponds and outdoor flat-panel photobioreactors. This vampyrellid amoeba was a significant grazer of *Scenedesmus* and was frequently associated with a very rapid decline in algal numbers. We report on the morphology, subcellular structure, feeding behavior, molecular phylogeny, and life cycle. The new amoeba resembles *Leptophrys* in the shape of trophozoites and pseudopodia and in the mechanism of feeding (mainly by engulfment). It possesses two distinctive regions in helix E10_1 (nucleotides 117 to 119, CAA) and E23_1 (nucleotides 522 and 523, AG) of the 18S rRNA gene. It did not form a monophyletic group with *Leptophrys* in molecular phylogenetic trees. We establish a new genus, *Vernalophrys*, with the type species *Vernalophrys algivore*. The occurrence, impact of the amoeba on mass culture of *S. dimorphus*, and means to reduce vampyrellid amoeba contamination in *Scenedesmus* cultures are addressed. The information obtained from this study will be useful for developing an early warning system and control measures for preventing or treating this contaminant in microalgal mass cultures.

Some green microalgae, species of *Scenedesmus*, are being explored for biomass production because they grow rapidly and synthesize large amounts of protein, starch, and lipid (1), as well as pigments (2, 3). The biomass can be used in wastewater bioremediation, carbon capture, animal feed, and biofuels (4). The use of *Scenedesmus* has been hampered by the difficulties in cultivating the alga on a commercial scale, caused in part by microbial contamination and losses due to microbial or zooplankton predators (5, 6).

The identification of microbial contaminants is a critical first step in developing an effective early warning system and control measures that prevent or treat contamination (7). Information about contaminants in *Scenedesmus* cultures is rather limited. Microbial contaminants reported in outdoor cultures of *Scenedesmus* include *Spirillum*-like bacteria (8); fungi, such as *Chytridium* (9) and *Amoeboaphelidium protococcarum* (7, 10, 11); and an opisthokont intracellular parasitoid, *Aphelidium* sp. (12, 13). In our environments in Arizona, amoebae, ciliates, and rotifers were the main eukaryotic contaminants in *Scenedesmus* cultures. In particular, a vampyrellid amoeba was found to have the most damaging impact, with the contamination of cultures by the amoeba often leading to rapid and almost complete loss of *Scenedesmus* in a few days.

Vampyrellids are a group of naked filose amoebae with distinctive morphologies, ultrastructure, and body forms that include amoeboid trophozoites, large plasmodia, and digestive cysts (14, 15). Since the initial studies in the 19th century (16–18), "vampire amoebae" have attracted attention because of their peculiar mode of feeding on algae, fungal spores, or hyphae. Some, like *Vampyrella lateritia*, cut holes in the walls of prey cells and suck up the cytoplasm of the prey through the hole (19). *Lateromyxa gallica* penetrates the cell wall to digest the cytoplasm of the prey (20), while still others, like *Arachnula impatiens* and *Theratromyxa weberi*, engulf whole prey by phagocytosis (21, 22). Vampyrellids have been suggested to have a role in suppressing organisms like fungi and nematode worms that cause plant diseases (23).

Almost 30 species of vampyrellid amoebae have been described in seven genera (*Arachnula*, Cienkowski 1876; *Gobiella*, Cienkowski 1881; *Lateromyxa*, Hülsmann 1993; *Leptophrys*, Hertwig and Lesser 1874; *Platyreta*, Cavalier-Smith 2008; *Theratromyxa*, Zwillenberg 1952; and *Vampyrella*, Cienkowski, 1865). They generally occur in soils and freshwater (14, 20), but some have been detected in marine habitats (24). Three further genera of filose algivorous amoebae have been reported, but one (*Vampyrellidium*, Zopf 1885) is related to the nucleariid filose amoebae, and the affinities of the other two (*Asterocaelum*, Canter 1973 and *Hyalodiscus*, Hertwig and Lesser 1874) have yet to be resolved.

Received 19 January 2015 **Accepted** 23 March 2015

Accepted manuscript posted online 27 March 2015

Citation Gong Y, Patterson DJ, Li Y, Hu Z, Sommerfeld M, Chen Y, Hu Q. 2015. *Vernalophrys algivore* gen. nov., sp. nov. (Rhizaria: Cercozoa: Vampyrellida), a new algal predator isolated from outdoor mass culture of *Scenedesmus dimorphus*. Appl Environ Microbiol 81:3900–3913. doi:10.1128/AEM.00160-15.

Editor: A. M. Spormann

Address correspondence to Yingchun Gong, springgong@ihb.ac.cn, or Qiang Hu, huqiang@ihb.ac.cn.

Supplemental material for this article may be found at http://dx.doi.org/10.1128/AEM.00160-15.

doi:10.1128/AEM.00160-15

Given the impact of this amoeba on the productivity of *Scenedesmus* cultures, we sought to identify it and to consider how best to manage it.

MATERIALS AND METHODS

Organism and culture conditions. *Scenedesmus dimorphus* (UTEX number 1237) was acquired from the Culture Collection of Algae at the University of Texas (Austin, TX) and grown in outdoor raceway ponds (ca. 600 liters) and flat-panel photobioreactors (1,600 liters) with a modified BG-11 culture medium (25, 26) at the Mesa, AZ, campus of Arizona State University.

Light microscopy. Observations and photomicrography were performed with differential interference contrast (DIC) using an Olympus BX51 microscope with an Olympus DP72 digital camera (Olympus, Japan). In order to record amoeba movement, feeding, and digestion processes, movies were also taken. About 10 ml of original algal cultures were taken for observation on all sampling events. Ingestion and digestion of *S. dimorphus* were examined using approximately 50 to 100 amoebae that had been picked up with micropipettes under a dissecting microscope and cultured in the presence of added *Scenedesmus* cells under laboratory conditions. Observations *in vivo* and with acridine orange (AO) staining were carried out 0 h, 2 h, 6 h, 12 h, 18 h, and 24 h after adding the algae.

Scanning and transmission electron microscopy. For scanning electron microscopy (SEM), hundreds of amoebae in different stages were picked up with micropipettes under dissecting microscopes and collected in 1.5-ml centrifuge tubes. The cell suspension was fixed with an equal volume of a phosphate-buffered saline (PBS) solution (0.01 M, pH 7.4) containing 4% glutaraldehyde and kept at 4°C for 2 h. One drop of the pellet from the bottom of the tube was placed onto a glass coverslip coated with 0.1% poly-L-lysine. Adhering cells were washed three times with PBS and postfixed with 1% osmium tetroxide in PBS for 1 h at room temperature. After three rinses in ultrapure water, samples were dehydrated in a graded acetone series and critical-point dried in a Balzers CPD020 using liquid carbon dioxide. The coverslips with attached cells were mounted on an aluminum stub and coated with approximately 15 nm of gold-palladium in a Technics Hummer-II sputter coater. Specimens were examined with a JEOL JSM-6300 scanning electron microscope operated at 15 kV.

For transmission electron microscopy (TEM), cells were harvested by gentle centrifugation (3,000 × *g* for 10 min; Eppendorf MiniSpin) and fixed with a PBS buffer (pH 7.4) containing 2% glutaraldehyde overnight at 4°C. After washing in PBS, cell samples were postfixed with 1% OsO_4 in PBS for 2 h at room temperature. Following a stepwise acetone dehydration and infiltration with Spurr's epoxy resin, the cell samples were embedded and polymerized in Spurr's epoxy resin at 60°C for 16 h. Ultrathin sections (65 nm) were cut using a Leica Ultracut-R microtome and double stained with 2% uranyl acetate and Sato's lead citrate (27). Specimens were examined with a Philips CM12 transmission electron microscope operated at 80 kV.

Staining for photomicroscopy. In order to stain the cell nucleic acid, amoebae were suspended in 0.05% AO solution for 5 min and then washed with phosphate-buffered saline (pH 7.0) prior to microscopic observation with a fluorescence microscope (BX51; Olympus) equipped with filter sets for blue and green excitation.

DNA amplification, sequencing, and phylogenetic analysis. About 100 amoeba cells at different stages were isolated from *Scenedesmus* cultures using fine glass pipettes and rinsed in distilled water three times to ensure no contaminants were carried over (28). The amoebae were then transferred to microcentrifuge tubes. Total DNA was extracted using a DNeasy Plant minikit (Qiagen, Hilden, Germany) following the supplier's instructions. In order to confirm that cells with different appearances were different stages of the same species, single-cell PCR amplification was performed for trophozoites, plasmodia, and digestive cysts by picking up one cell and putting it in a PCR tube. Usually, 10 replicates were done for these stages. Because very few resting cysts were present, the information about this stage is from live microscopic observations alone.

The small-subunit (SSU) rRNA gene sequence was amplified using Lucigen (Middleton, WI) Econo *Taq* Plus Green 2× and universal forward primers A (5′-AACCTGGTTGATCCTGCCAGT-3′ [29]) and LSUR (5′-GTTAGTTTCTTTTCCTCCGC-3′ [30]). Temperature cycling was set as follows: an initial denaturation step at 95°C for 5 min, and then 35 cycles of 95°C for 30 s, 54°C for 30 s, and 72°C for 2 min, followed by a final elongation step of 72°C for 10 min. Reactions were performed in a Perkin-Elmer GeneAmp PCR System 9600 (PE Applied Biosystems, Mississauga, ON, Canada). The individual PCR products were purified with a QIAquick gel extraction kit (Qiagen, Hilden, Germany) and then ligated separately into TOPO vector with a TOPO cloning kit (Invitrogen, California) and transformed into Top 10 competent cells. For single-cell PCR products, one positive clone was selected from each picked cell amplification product, taking into consideration that the single-cell PCRs sometimes failed, and finally, 5 to 10 positive clones from each putative life stage, i.e., trophozoite, plasmodium, and digestive cyst, were selected, while for the PCR products from DNA extractions, 10 positive clones were selected to isolate plasmid DNA with a QIAprep Spin Miniprep kit (Qiagen, Hilden, Germany). These were then sequenced using a BigDye Terminator v3.1 in an ABI Prism 3730 genetic analyzer (Applied Biosystems, Perkin-Elmer Corp., United Kingdom). Two primers were specifically designed for sequencing: forward primer 792F (5′-GCTTGAATGCGTT AGCATGG-3′) and reverse primer 1539R (5′-CATCGTGATGGGGTTT GACGAT-3′).

For phylogenetic analysis, multiple alignments of sequences were performed using ClustalX (31) and then manually arranged with SeaView (32). The alignment analyses were conducted with Mega 6 (33) to determine any unique nucleotide regions for the amoeba, and the SSU rRNA secondary structure of *Tetrahymena canadensis* (accession number M26359 [http://bioinformatics.psb.ugent.be/webtools/rRNA/secmodel/Tcan_SSU.htm]) was set as a reference. Aligned sequences were analyzed using maximum likelihood (ML) (34), maximum parsimony (MP) (35), neighbor joining (NJ) (36), and Bayesian inference (BI) (37). The four topologies were inferred using the model selected as the best-fit model of nucleotide substitution by AIC in Modeltest 3.7 (38) and implemented in PAUP 4.0b10. MP and NJ phylogenetic analyses were performed with PAUP* 4.0 (39), while ML phylogenetic analyses were carried out online (http://atgc.lirmm.fr/phyml/) and the BI method was conducted with MrBayes 3.0b (37, 40). All parsimony, likelihood, and distance data were bootstrap resampled 1,000 times, and for the Bayesian analysis, the chain length for our analysis was 1,000,000 generations, with trees sampled every 100 generations, and the first 4,000 generations were discarded as burn in.

Assessment of the impact of *Vernalophrys algivore* on *Scenedesmus* cultures. We surveyed *S. dimorphus* cultures for contaminants over 3 years (2010 to 2013). From 16 to 20 August 2012, we conducted quantitative studies on three panels of cultures in outdoor photobioreactors (1,600 liters) that were contaminated with the amoebae. At the same time, we monitored three panels of uncontaminated cultures as controls. Three replicates of 50 ml were taken from each culture each day and fixed with Lugol's solution (1% final concentration) for cell counts. Under a light microscope (BX51; Olympus, Japan), algal numbers were determined using a hemocytometer (Hausser Scientific, Horsham, PA, USA), and the concentration of the contaminated amoebae was measured with a Nageotte Counting Chamber (0.1 ml; Hausser Scientific, Horsham, PA, USA). The data were analyzed using Microsoft Excel 2007. Ingestion rates were determined by the disappearance of algae using the following formula: $\mathrm{Ic} = \Delta P/F \times \Delta t = \Delta P/[(F_2 - F_1)/(\ln F_2 - \ln F_1)] \times \Delta t$, where ΔP is the decrease in prey cell numbers during time interval Δt and F_2 and F_1 are the predator cell densities (cells · ml^{-1}) at the end and beginning, respectively, of each interval (41).

Nucleotide sequence accession number. The complete SSU rRNA gene sequence of the vampyrellid was submitted to GenBank under accession no. KF141791.

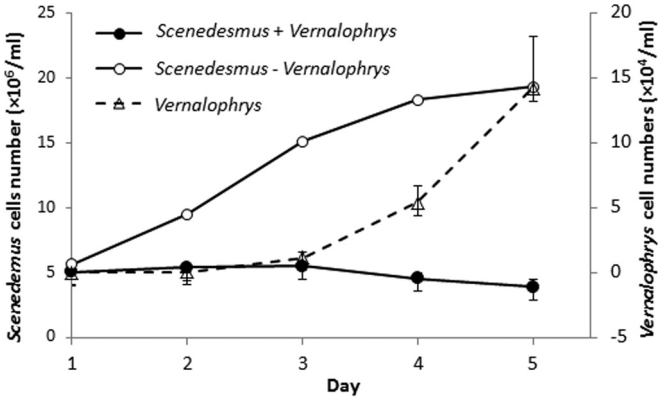

FIG 1 Data on the growth of *S. dimorphus* in outdoor photobioreactors (1,600 liters) from 16 to 20 August 2012. Axenic cultures of *S. dimorphus* infected with *V. algivore* failed to grow and decreased over time (●), while the numbers of *V. algivore* cells increased (△). Uninfected controls showed the familiar lag, log-, and stationary-phase changes in algal cell numbers (○).

RESULTS

The presence of vampyrellids caused deterioration or collapse of *Scenedesmus* cultures. Over 3 years (2010 to 2013) of surveys, the numbers of *S. dimorphus* organisms raised in outdoor ponds or photobioreactors were sometimes reduced quickly, leading to a significant drop in productivity. Microscopic inspection of these cultures revealed the presence of the amoeba, distinguished as a vampyrellid because of the shape of the cell, pseudopodia, and the presence of surface granules. Field data that illustrate the impact of the predator on *S. dimorphus* in photobioreactors are shown in Fig. 1. When *S. dimorphus* was free of contamination by the vampyrellid or its concentration was too low to be observed, the growth of *Scenedesmus* cells followed a typical sigmoid growth pattern, achieving yields in excess of 10^7 cells/ml (Fig. 1, open circles). However, if vampyrellids occurred in the cultures, the *S. dimorphus* population remained unchanged for approximately the first 2 days, and then the numbers gradually declined (Fig. 1, solid circles). Under these circumstances, the number of vampyrellid amoebae increased considerably (Fig. 1, triangles). The inverse correlation between the *Scenedesmus* and vampyrellid populations led to the hypothesis that the vampyrellid was a grazer and was responsible for the reduction of the *Scenedesmus* populations. The maximum vampyrellid populations can be as high as 1.8×10^5 cells ml^{-1}, and their grazing rate was as high as 154 *Scenedesmus* cells day^{-1} $individual^{-1}$ (based on data from day 3 to day 5 in Fig. 1).

During our survey, contamination of *Scenedesmus* cultures by the amoebae occurred at any time of the year, including hot summers (about 40°C) and winters (close to 4 to 5°C), but in particular in the summer months. The vampyrellid was found only in outdoor photobioreactors or open raceway ponds and was never found in indoor cultures in glass columns (5-cm diameter and 1-liter culture volume) or with any other algal species that were being cultured, including the freshwater *Chlorella zofingiensis* and the marine *Nannochloropsis oceanica*.

We tried to isolate single vampyrellid cells and cultivate them in the presence of *Scenedesmus* cells under laboratory conditions but were unable to achieve the high numbers we observed in the outdoor *Scenedesmus* cultures.

Morphology and ultrastructure of the vampyrellid. (i) Light microscopy (LM). Four forms of the species were observed: motile feeding trophozoites (Fig. 2A to C), larger multinucleated plasmodia (Fig. 2D), digestive cysts (Fig. 2E to G), and resting cysts (Fig. 2I). Sometimes, dumbbell-shaped cysts (Fig. 2H) were observed.

Trophozoite cells ranged in diameter from 10 to 30 μm and were typically flattened and fan shaped (Fig. 2A and B), typical of expanded vampyrellids (14). The filopodia were up to 50 μm long, thin, tapering, and mostly unbranched. They arose from a frontal or frontolateral hyaline and very delicate fringe of the cytoplasm (Fig. 2A). No granules occurred on the filopodia. The cortical cytoplasm was hyaline and colorless. Many inclusions occurred in the endoplasm (Fig. 2A and D), and small refractile granules lay just below the cell surface (Fig. 2D). Sometimes, numerous vacuoles were present, predominantly in the peripheral cytoplasm (Fig. 2C).

The cells moved smoothly over a surface, and movement was accompanied by retraction of the filopodia (see Movie S1 in the supplemental material). Occasionally, individuals attached to a substrate with broader pseudopodia (Fig. 2C). Due to the dense matrix of the central cytoplasm, it was not usually possible to discriminate distinct organelles, such as nuclei and contractile vacuoles. Occasionally, two contractile vacuoles were visible in newly formed plasmodia (Fig. 2D).

Plasmodia occurred in *Scenedesmus* cultures with high numbers of trophozoites. They formed when small trophozoites fused (Fig. 2D). Larger plasmodia with diameters of 20 to 300 μm or more appeared as the result of two or several fusions between smaller and formerly independent individuals. During the formation of plasmodia, individuals combined their cytoplasm immediately after contact with each other. Filopodia of plasmodia can radiate from all sides but remain rather inactive, soft, and slender (Fig. 2D).

The sizes of digestive cysts varied from 30 to 100 μm, depending on the amount of food they contained. Usually, the cyst outlines were spherical or slightly elliptical (Fig. 2E and F). Occasionally, some elongate and irregular digestive cysts (Fig. 2G) were observed, and they seemed to have formed from larger plasmodia.

Resting cysts (Fig. 2I) with a size of 20 to 35 μm were observed occasionally in the summer season even in the presence of food. Because very few resting cysts were observed during our study, we do not have detailed information about them. The major difference between the digestive cyst and the resting cyst was that the latter had a thicker envelope covering the cytoplasm (Fig. 2I).

(ii) SEM. SEM revealed more detailed information about the cell surfaces of trophozoites (Fig. 3A to F) and digestive cysts (Fig. 3G to L). The prominent structures on the surfaces of the trophozoites were thin filopodia (Fig. 3A to C) and dome-shaped structures (Fig. 3A, B, and D to F). Usually, filopodia were slender, bent, and short and projected directly from the cell surface (Fig. 3B). Sometimes they appeared to be branched, especially when the trophozoites captured algal cells (Fig. 3C). The dome-shaped structures were less evident when the trophozoites were covered with many filopodia (Fig. 3A and B) but were more obvious when there were fewer filopodia (Fig. 3D to F).

Digestive cysts were distinguished by having an organic cyst wall (Fig. 3G and J to L) and some material that made algal cells adhere to the amoeba surface (Fig. 3G to L) and even disrupt and fuse normal or empty algal cells (Fig. 3G to I and K).

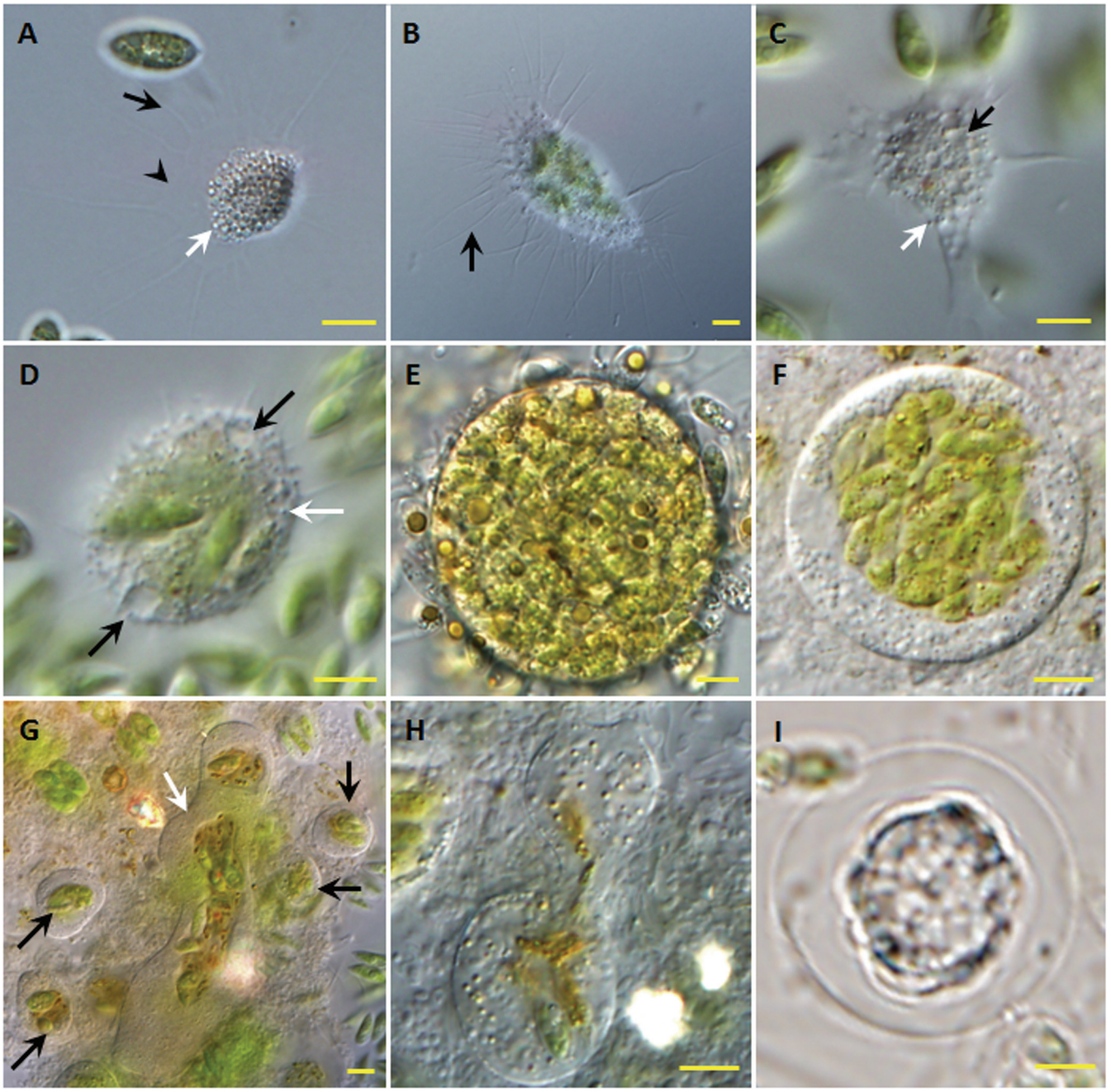

FIG 2 Forms and morphological traits of *V. algivore* gen. nov., sp. nov. (DIC optics). (A) Advancing trophozoite with an expanded morphotype; long, thin, tapering, and mostly unbranched pseudopodia (black arrow) arise from a hyaline and very delicate fringe of the cytoplasm (arrowhead), and there are many inclusions (white arrow) inside the cell body. (B) Advancing trophozoite with ingested *Scenedesmus* cells; the pseudopodia (arrow) arise from a delicate fringe of cytoplasm. (C) Cell with numerous vacuoles (black arrow) and peripheral granules (white arrow). (D) Forming plasmodium with two contractile vacuoles (black arrows); small refractile granules (white arrow) lie just below the cell surface, and there is no thin hyaloplasm. (E) Large early digestive cyst with many *Scenedesmus* cells located throughout the cell. (F) Large digestive cyst in the middle stage, in which the ingested algal cells have moved to the center of the amoeba. (G) Digestive cysts with different shapes; most are small and round with centralized food (black arrows), and one large digestive cyst is elongate and irregular (white arrow) with a central mass of food. (H) Digestive cysts in division. (I) Resting stage. Scale bars = 5 μm.

(iii) TEM. Early digestive cysts contained many small food vacuoles (Fig. 4A), but as digestion progressed, the food vacuoles were combined into a large one (Fig. 4B and C). Digestive cysts had an extra external layer (Fig. 4D) compared to trophozoites (Fig. 4F).

The cytoplasm of trophozoites was mainly composed of lipids and starches (Fig. 4E), and there were more mitochondria than in digestive cysts (Fig. 4B and E). Most contained a single spherical nucleus (2- to 3-μm diameter) (Fig. 4A and 5A and B) with a central condensed nucleolus (ca. 0.3 μm) (Fig. 5A) similar to that of *Leptophrys* (15). The mitochondria had tubular/saccular cristae (Fig. 5B and E) and were distributed throughout the cytoplasm

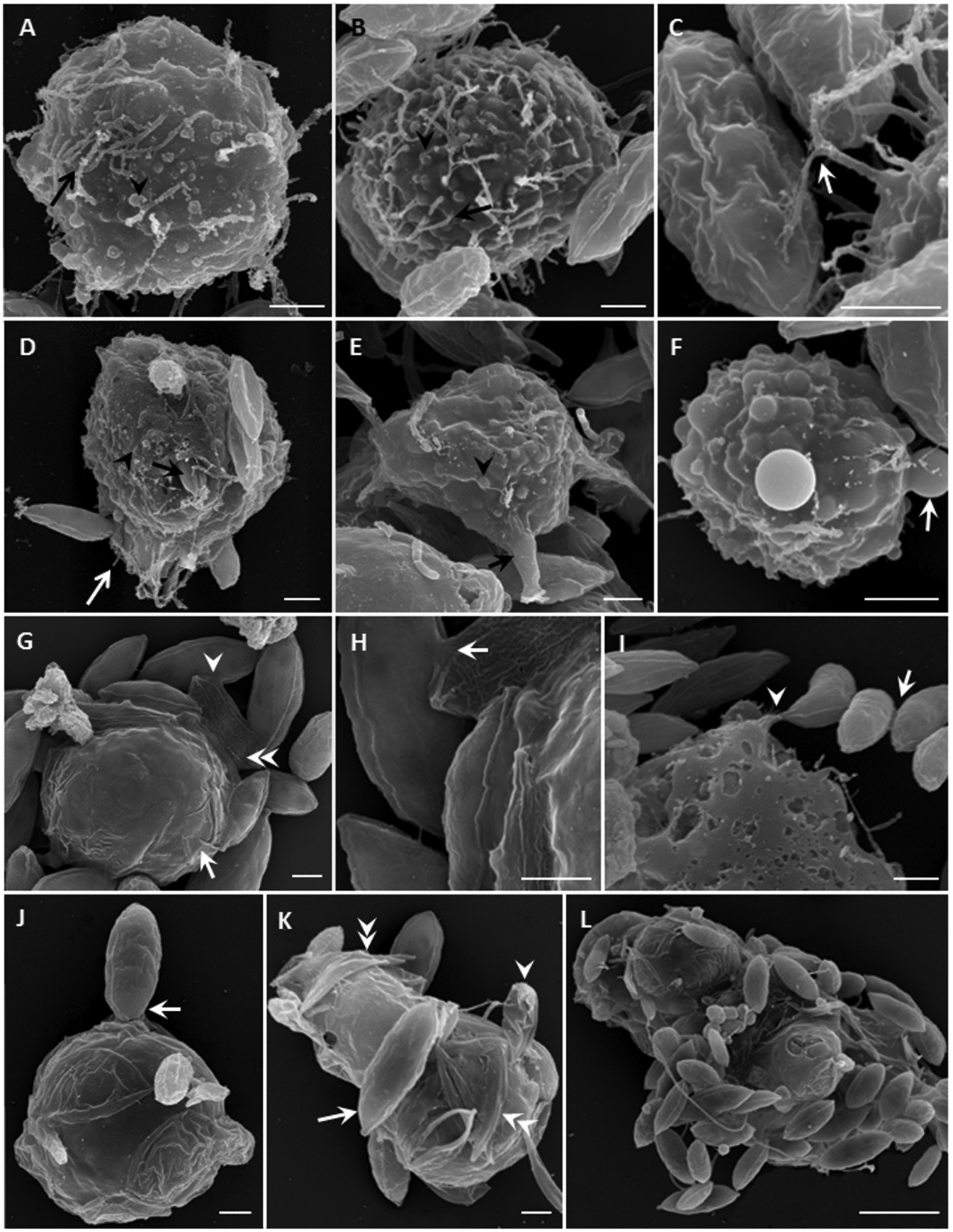
A
B
C
D
E
F
G
H
I
J
K
L

(Fig. 5E). The dictyosomes usually had about 5 cisternae (Fig. 5D). A concentric membrane structure (Fig. 5B and C) that was observed near the nucleus may be that of a Golgi apparatus.

Feeding characteristics of the vampyrellid. As shown in Movie S2 in the supplemental material, which was taken by time lapse, trophozoites and plasmodia can engulf *Scenedesmus* using filopodia (Fig. 6A). Algal cells tended to adhere to plasmodia (Fig. 6B) or early digestive cysts (Fig. 3G to L). Large flocs (Fig. 6E) composed of many digestive cysts, or perhaps some trophozoites and plasmodia, were typical in contaminated *Scenedesmus* cultures. They helped to aggregate algal cells and facilitated grazing by the amoebae. Sometimes, it was observed that one *Scenedesmus* cell was being ingested by a digestive cyst (Fig. 3J and 6C). Since this phenomenon is unusual and glutaraldehyde, which we used as a fixative, is a "sticky" chemical and may have caused some adhesion of algae and amoebae, the feeding characteristic where the digestive cyst can ingest algal cells needs to be confirmed in future studies.

Usually it took the amoeba several hours to 24 h to complete the capture, ingestion, and digestion of algal cells (Fig. 7). The process was accompanied by a change in the color of the amoeba (Fig. 7). In early stages of digestion, the ingested algal cells appeared green (Fig. 6D, black arrow, and 7, 6 and 12 h) and were distributed throughout the digestive cysts (Fig. 2E and 6A). As digestion proceeded, the ingested algal cells turned brown or orange, were pushed toward the center of the amoeba (Fig. 6D, white arrow, and 7, 12 h), and were surrounding by colorless or slightly orange cytoplasm (Fig. 6D, white arrow, and E). In the late stages of digestion, only some brown remnants were left in the food vacuoles (Fig. 7, 18 and 24 h). After digestion, the amoeba exits the cyst, leaving some remnants behind (Fig. 6D, arrowhead).

In the early stages of digestion, algal cells had complete cell walls and intact subcellular organelles (Fig. 5G)—almost the same as normal algal cells (Fig. 5F). As feeding continued, the algal walls showed signs of damage (Fig. 5H to I). The amoebae seemed unable to digest the algal walls, since many remained in food vacuoles at the middle and late stages of digestion (Fig. 4B and C) or were expelled from the amoeba into the environment (Fig. 5I). Lipid droplets and starch granules are energy storage products in *Scenedesmus* cells (Fig. 5F). Some lipid droplets in digestive cysts (Fig. 5J and K) were larger than in regular algal cells (Fig. 5F), suggesting that the lipids can fuse during digestion. The amoebae do not always digest lipids and starches completely, with many found outside the food vacuoles (Fig. 4B and C and 5M) and even appearing to be released from food vacuoles into the cytoplasm (Fig. 5L).

Molecular phylogenetic characterization of the vampyrellid. In total, 30 colonies derived from trophozoites, plasmodia, digestive cysts, and the mixed cells in different life stages were used for sequencing. Nine partial SSU rRNA gene sequences with minor differences (0- to 7-nucleotide differences among 665 nucleotides [see Fig. S3 in the supplemental material]) were obtained, and three colonies were further used to do sequencing to get the complete SSU rRNA gene sequence of the vampyrellid, which comprised 1,809 bp with a GC content of 45.4%. In order to conduct comparative analyses, 47 SSU rDNA sequences, including all the available 18S rRNA gene sequences (36 species or strains; >1,000 bp) from Vampyrellida and 8 representative sequences from Phytomyxea, Ascetosporea, and Gromiidea, were used to construct the phylogenetic tree. Three members of Chlorarachniophyceae were used as outgroups. As some species were represented by partial SSU rRNA gene sequences, we used 1,005 bp of the SSU rRNA gene sequences for the analysis. The numbers of conserved, variable, and parsimony-informative sites among all Leptophryidae, Vampyrellidae, and three unclassified vampyrellids were 704 (70.0%), 294 (29.3%), and 235 (23.4%), respectively. Two distinctive regions in the sequence were detected in the new vampyrellid (Fig. 8). The first was CAA (nucleotides 117 to 119) in helix E10_1, while at this position the bases are UUU in *Leptophrys*, UAA for the soil dweller group of *Arachnula-Theratromyxa-Platyreta*, and NUU for *Vampyrella*. The second was AG (nucleotides 522 and 523) in helix E23_1, while at this position it is GA for *Leptophrys* and GG for the group of *Arachnula-Theratromyxa-Platyreta* and *Vampyrella* (Fig. 8).

Phylogenetic analyses were done using the ML, MP, NJ, and BI methods, and both the two-tailed Wilcoxon signed-rank test and the Kishino-Hasegawa (KH) test (see Table S4 in the supplemental material) showed that topologies inferred from BI and ML were the best. As the two topologies were nearly identical, both were incorporated into a consensus tree based on the ML tree (Fig. 8).

Our expanded data set strongly confirmed the monophyly of vampyrellids and their position as a sister group to Phytomyxea, Ascetosporea, and Gromiidea within the Endomyxa part of phylum Cercozoa (Fig. 8) (90% and 0.95 by ML and BI). Similar to the study of Berney et al. (24), three main clades (A, B, and C) of vampyrellids were recovered (Fig. 8). Clade A comprises only sequences derived from organisms of nonmarine (soil, freshwater, and moss-associated) habitats; the sequences of clade B were from both marine and terrestrial environmental libraries, some from basically freshwater sites with high levels of dissolved minerals; clade C is strongly supported and is a robustly basal sister lineage to A and B. Our vampyrellid, a freshwater species, was located within clade A (Fig. 8) and was close to the members of the Leptophryidae, such as *Arachnula*, *Theratromyxa*, and *Platyreta*. Our vampyrellid grouped with two environmental cercozoan isolates

FIG 3 Scanning electron micrographs of *V. algivore*. (A) Trophozoite, with many thin and long filopodia (arrow) and some retracted filopodia that became dome-shaped structures (arrowhead). (B) Larger trophozoite, with some filopodia (arrow) and more dome-shaped structures (arrowhead). (C) Detail of how filopodia capture prey; the arrow shows where the filopodium appears branched. (D) Trophozoite with shorter filopodia (white arrow) and some dome-shaped structures (arrowhead); one *Scenedesmus* cell (black arrow) is being engulfed. (E) Trophozoite with thick filopodia (arrow) and more dome-shaped structures (arrowhead). (F) Trophozoite with significant dome-shaped structures (arrow) on the surface of the cell. (G) Digestive cyst surrounded by an organic cyst wall (arrow), which was covered by *Scenedesmus* cells; in some, only an empty cell remained (double arrowheads). Algal cells can be connected to each other (arrowhead). (H) Detail of panel G showing that the cell walls were disrupted and fused (arrow). (I) Four *Scenedesmus* cells outside the amoeba were connected by unknown material (arrow), and one of them was connected by the cell inside the amoeba (arrowhead). This might be an artifact of preparation but is consistent with the information in Fig. 5H. (J) Round digestive cyst with thin membrane and one *Scenedesmus* cell adhering to the surface (arrow). (K) Large and irregular digestive cyst with some *Scenedesmus* cells, showing one cell (arrow) adhering to the surface, one shrunken cell submerged in the body (arrowhead), and several empty cells beneath the thin membranes (double arrowheads). (L) Large irregular digestive cyst with many adhering *Scenedesmus* cells. Scale bars = 2 μm (A to K) and 10 μm (L).

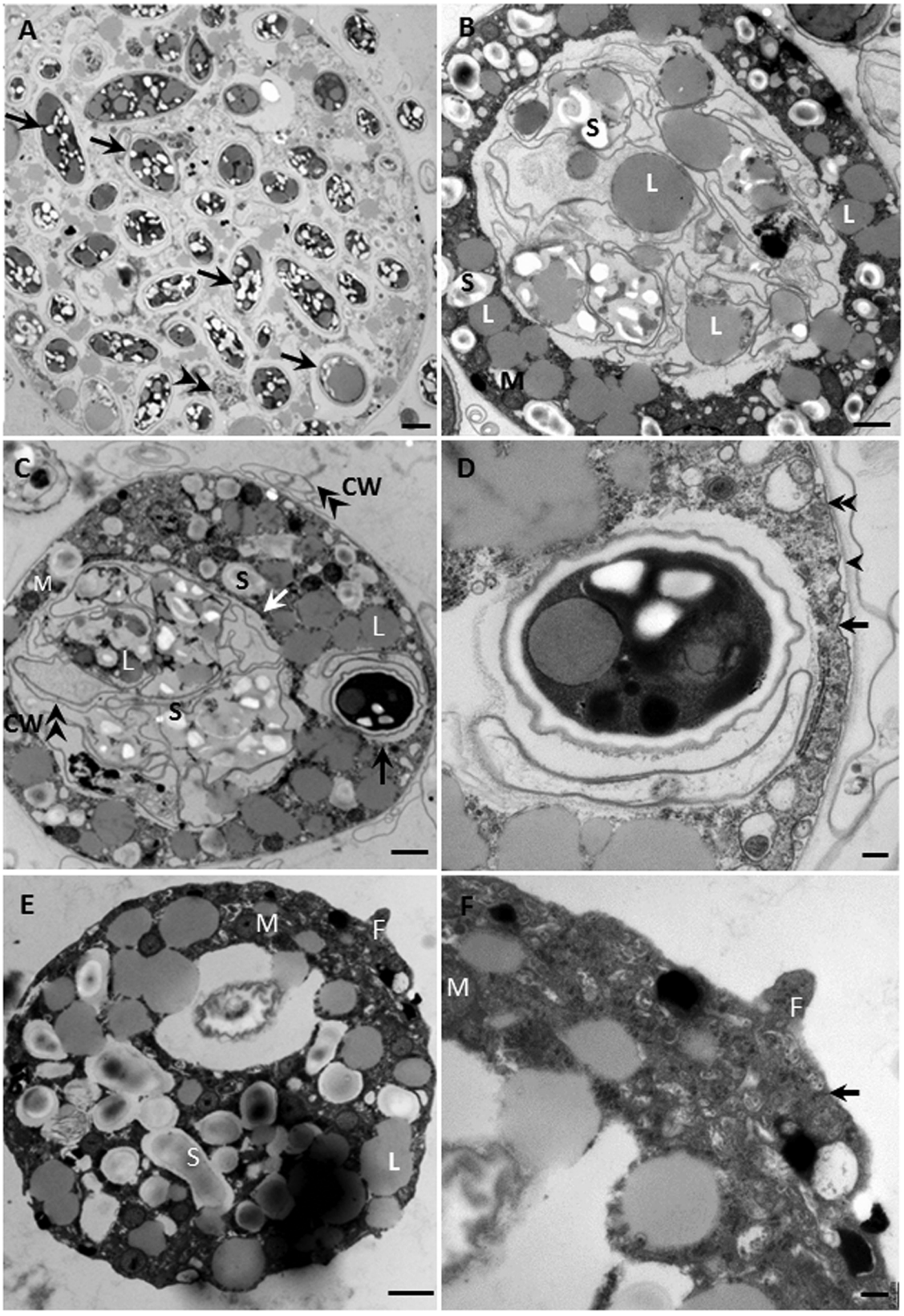

FIG 4 Transmission electron micrographs of thin-sectioned *V. algivore*. (A) Newly formed digestive cyst with many intact algal cells (arrows) inside the body and one nucleus (double arrowheads). (B) Middle-stage digestive cyst with one large food vacuole in the center of the body and lipids (L) and starch (S) distributed both inside and outside the food vacuole. (C) Late-stage digestive cyst with one large food vacuole (white arrow) and a newly formed food vacuole (black arrow); many algal cell walls (double arrowheads) lie inside the old vacuole, and some lie outside the cell. CW, cell wall; M, mitochondrion. (D) Detail of cell in panel C showing a digestive cyst with one intact *Scenedemus* cell with the cell membrane (arrow) and a cyst envelope (arrowhead); in some regions (double arrowheads), the cyst and the plasma membrane adhere to each other. (E) Trophozoite with many mitochondria, lipid, and starch inclusions. F, filopodium. (F) Detail of pseudopodium in panel E. There is a single membrane around the trophozoite, and the electron density of the filopodium is similar to that of the cytoplasm. Scale bars = 2 μm (A), 1 μm (B, C, and E), and 0.2 μm (D and F).

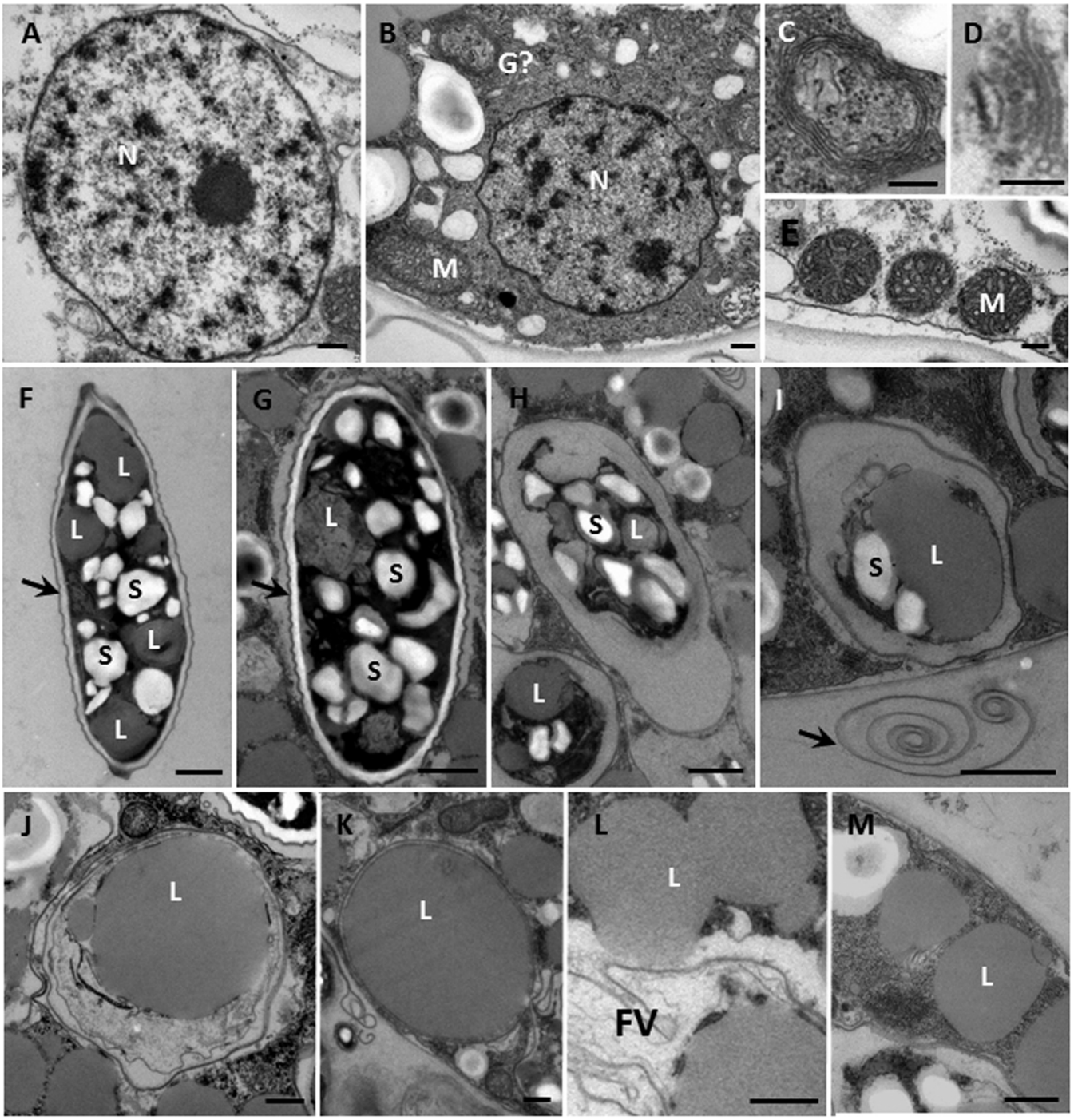

FIG 5 Transmission electron microscopy. (A) Nucleus (N) of a digestive cyst; detail of Fig. 4A showing the central nucleolus. (B) Nucleus of another digestive cyst, with a mitochondrion (M) and a membranous structure (perhaps a Golgi body) (G). (C) Detail of the membranous structure in panel B. (D) Golgi apparatus; dictyosome with 5 sacs. (E) Mitochondria of trophozoite with tubulovesicular cristae. (F) Live *Scenedesmus* cell, with intact cell wall (arrow), lipid droplet (L) (average size, 1.2 μm by 1.2 μm), and starch particles (S). (G) Newly ingested intact algal cell in a food vacuole with intact cell wall (arrow). (H) Ingested prey cell in which the wall is breaking down. (I) Food vacuole with only starch and lipid; the arrow indicates some algal cell wall materials outside the amoeba. (J) Lipid droplet measuring 2.2 μm by 2.2 μm in a food vacuole. (K) Food vacuoles containing only a lipid droplet measuring 2.8 μm by 3.4 μm. (L) Detail of Fig. 4B suggesting that lipid is being released from a food vacuole (FV). (M) Lipid droplets near the cell surface. Scale bars = 0.2 μm (A to E), 1 μm (F to I), and 0.5 μm (J to M).

from anoxic sediments (24) with bootstrap values of 57% and 0.96 (ML/BI).

Possible life cycle. The molecular analysis confirms the light microscopic observations that the amoeba can exist with a variety of body forms with almost 99% genotypic similarities (the resting stage was not included). We have constructed a potential life cycle on the basis of the transitions we observed (Fig. 9). We begin with the trophozoite or feeding stage (Fig. 9A), as it is most abundant.

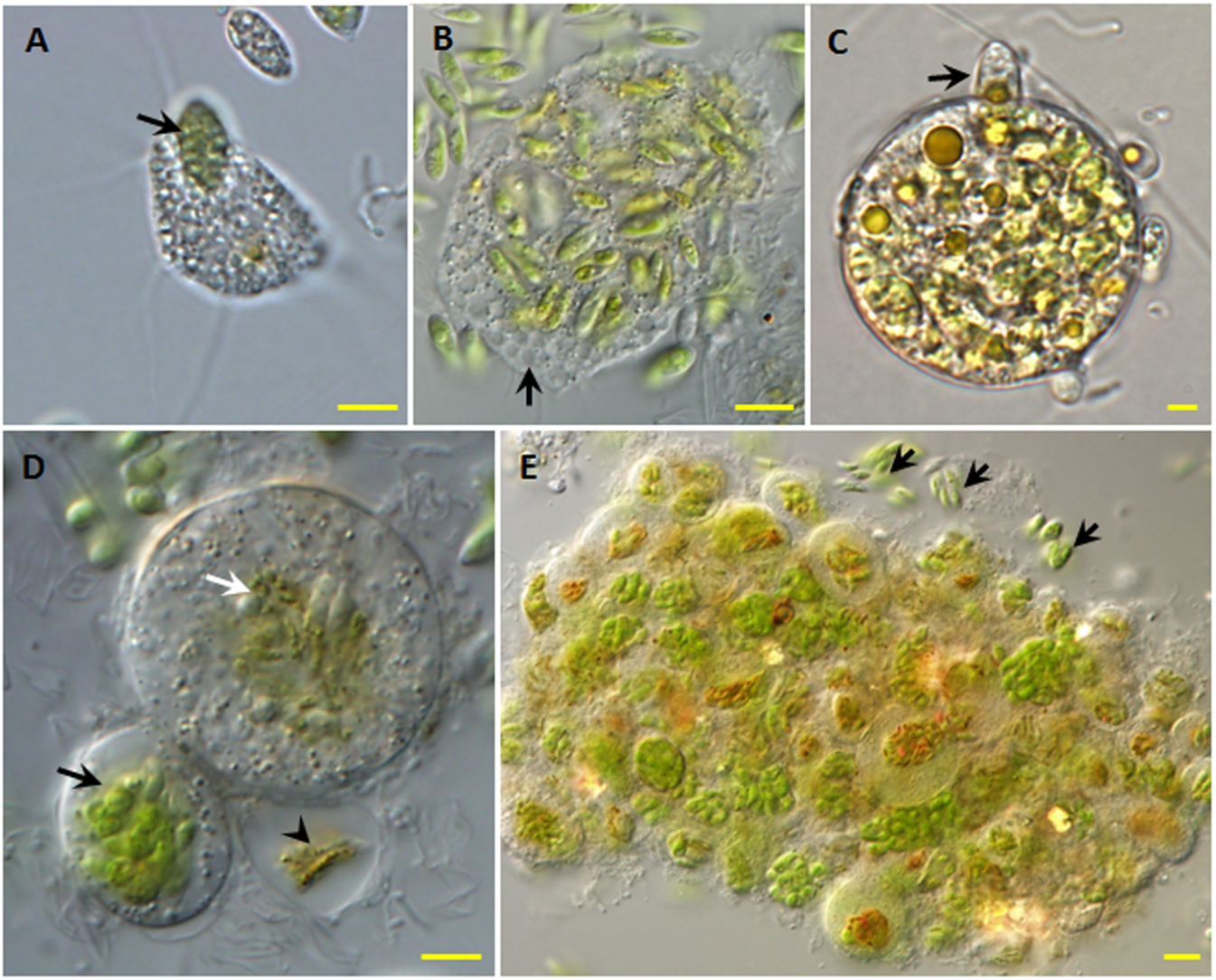

FIG 6 Feeding by *V. algivore* on *Scenedesmus* cells. (A) A *Scenedesmus* cell (arrow) is engulfed by a trophozoite. (B) Several *Scenedesmus* cells adhere to the surface of a plasmodium that has numerous vacuoles (arrow) in the cytoplasm. (C) One *Scenedesmus* cell (arrow) is ingested by an early-stage digestive cyst. (D) Digestive cysts in different stages; the small one (lower left) is in an early stage, and the engulfed cells (black arrow) are green and intact, while the large one is in a late stage and the ingested algal cells (white arrow) are near the center and are brownish. An empty cyst with some remnants of algal cells (arrowhead) has adhered to the large cyst. (E) Large floc with about 50 digestive cysts in different sizes and stages; the arrows point to some *Scenedesmus* cells that adhere to the floc. Scale bars = 5 μm (A to D) and 10 μm (E).

Trophozoites consume *Scenedesmus* cells mainly by engulfing them, and depending on their recent feeding history, their bodies are often full of ingested algal cells (Fig. 9B). We have observed trophozoites fusing to form what we refer to as plasmodia (Fig. 9C), a form that is also able to feed. Both the trophozoite and plasmodium can transform into digestive cysts (Fig. 9D), for which we showed little or no feeding. Digestive cysts formed from trophozoites were normally spherical, but those formed from plasmodia were sometimes elongate and irregular (Fig. 9E). During digestion, food moved to the center of the digestive cyst (Fig. 9F). After digestion, we presume that, as with other vampyrellids, such as *L. gallica* (21), an additional cell wall may be secreted and the digestion cyst transforms into a resting cyst (Fig. 9G). Excystation is presumably stimulated by the proper conditions (Fig. 9H), so that the amoeba returns to the trophozoite form.

Cell divisions have been reported for several genera of vampyrellids (15, 20); however, we did not observe any obvious cell division phenomenon for *V. algivore*. Probably, this was because the amoebae were often full of algal cells, which made it very difficult to observe the cytokinesis within the cells. We envisioned several possible cell division methods based on the characteristics of the related species. As observed in *Vampyrella*, *Gobiella*, and *Hyalodiscus* (15), the cytoplasm may divide in a digestive cyst (Fig. 9J), or as observed in *Leptophrys* (15), cell division may take place during excystation and then return to the feeding form (Fig. 9I). Furthermore, as with *Lateromyxa* (20), cell division may also occur in the trophozoite or plasmodium stage.

TAXONOMY

Vernalophrys, gen. nov., Gong, Patterson, and Hu, is a limnetic vampyrellid amoeba feeding by engulfment of unicellular chlorophy-

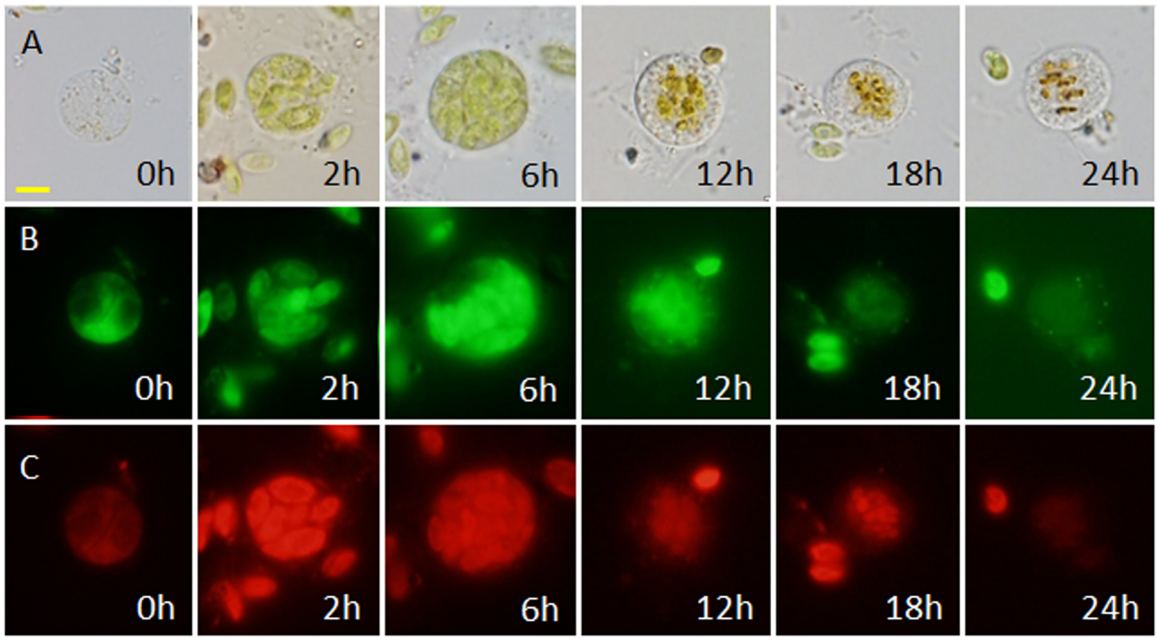

FIG 7 Ingestion and digestion of *S. dimorphus* cells by *V. algivore* at different times after feeding. Six cells are shown by light microscopy (A), DNA fluorescence (acridine orange staining) (B), and chlorophyll fluorescence (C). Scale bars = 5 μm.

cean algae (e.g., *Scenedesmus dimorphus*). It can exist as a trophozoite, plasmodium, digestive cyst, and resting cyst. The trophozoite predominantly exhibits an expanded fan-shaped appearance, with thin, tapering filopodia originating from the frontal or frontolateral hyaline fringe of the cytoplasm. Trophozoites, plasmodia, and digestive cysts can aggregate to form flocs. On the basis of the SSU rDNA gene sequence, this vampyrellid has closer affinities to *Leptophrys*, *Platyreta*, and other leptophryids than to the family Vampyrellidae; however, it has two distinctive regions in helix E10_1 (nucleotides 117 to 119; CAA) and E23_1 (nucleotides 522 to 523; AG) that made it different from the known leptophryids. The type strain was isolated from cultivation of *Scenedesmus* in both raceway ponds and flat-panel photobioreactors in Mesa, Arizona, USA. ZooBank identifier: urn:lsid:zoobank.org:act:949CB818-B9E4-4B50-8BF0-E1FBEDF9A15A. Type species: *Vernalophrys algivore*.

Vernalophrys algivore, sp. nov., Gong, Patterson, and Hu, possesses properties of the genus *Vernalophrys*. Trophozoites were 10 to 30 μm, plasmodia were 20 to 300 μm, digestive cysts were 30 to 100 μm, and resting cysts were 20 to 35 μm long. The type species was isolated from cultivation of *Scenedesmus* in both raceway ponds and flat-panel photobioreactors in Mesa, Arizona, USA. ZooBank I: urn:lsid:zoobank.org:act:7C1C1087-D658-423A-A260-0E8253AABEA9. Because of the nature of this species, we are unable to use a single specimen or preparation of a single specimen as type material and so designate EM blocks (20121002-TEM-SD-vampyrellid; 20120913-TEM-SD-vampyrellid; 20120906-SEM-SD-vampyrellid; 20130111-SEM-SD-vampyrellid) located at the Laboratory for Algae Research and Biotechnology, College of Technology and Innovation, Arizona State University, Mesa, Arizona, USA, as hapantotype, and the live amoeba samples with *Scenedesmus* cells were kept in both the Arizona State University and the Institute of Hydrobiology, Chinese Academy of Sciences, Wuhan, China. Type locality: Mesa, Arizona, USA.

DISCUSSION

The identification, taxonomy, and characteristics of *V. algivore*. Because of its distinctive characteristics, discussed below, the amoeba could be identified as a vampyrellid amoeba, but not as a known species. It is presented here as a new genus and species, *Vernalophrys algivore* gen. nov., sp. nov.

Algivory, the appearance of filopodia, the granular surface cytoplasm, the formation of plasmodia and digestive cysts, the ultrastructures of nuclei and mitochondria (vesiculate cristae), and molecular comparisons establish that the amoeba that contaminates the algal cultures is a vampyrellid. There are currently two families of vampyrellids, the Vampyrellidae and Leptophryidae (14), and seven genera. All have been reported from soil and freshwater (see Table S5 in the supplemental material). Moreover, three other genera of algivorous amoebae with filose pseudopodia (*Vampyrellidium*, *Hyalodiscus* and *Asterocaelum*) have been described (15, 42–44), but their affinities are not with vampyrellids or have yet to be resolved (see Table S5 in the supplemental material).

The following features of *V. algivore* are shared with other Leptophryidae (14): (i) the morphotype has an expanded creeping form (Fig. 2A and B); (ii) the pseudopodia are thin, tapering, and often emerging from hyaloplasmatic fringes at the cell margins (Fig. 2A and B); and (iii) the mechanism of food acquisition is primarily engulfment. Due to these shared morphological characteristics and close molecular similarity to known members of the Leptophryidae (Fig. 8), it is reasonable to assign *V. algivore* to the family Leptophryidae.

Four genera were included in the Leptophryidae by Hess et al. (14): *Arachnula*, *Leptophrys*, *Platyreta*, and *Theratromyxa*. *Vernalophrys* is most similar to *Leptophrys* in the shapes of the trophozoite and pseudopodia (Fig. 2A and B) and in the form of feeding (mainly engulfment), but it does not form a monophyletic group

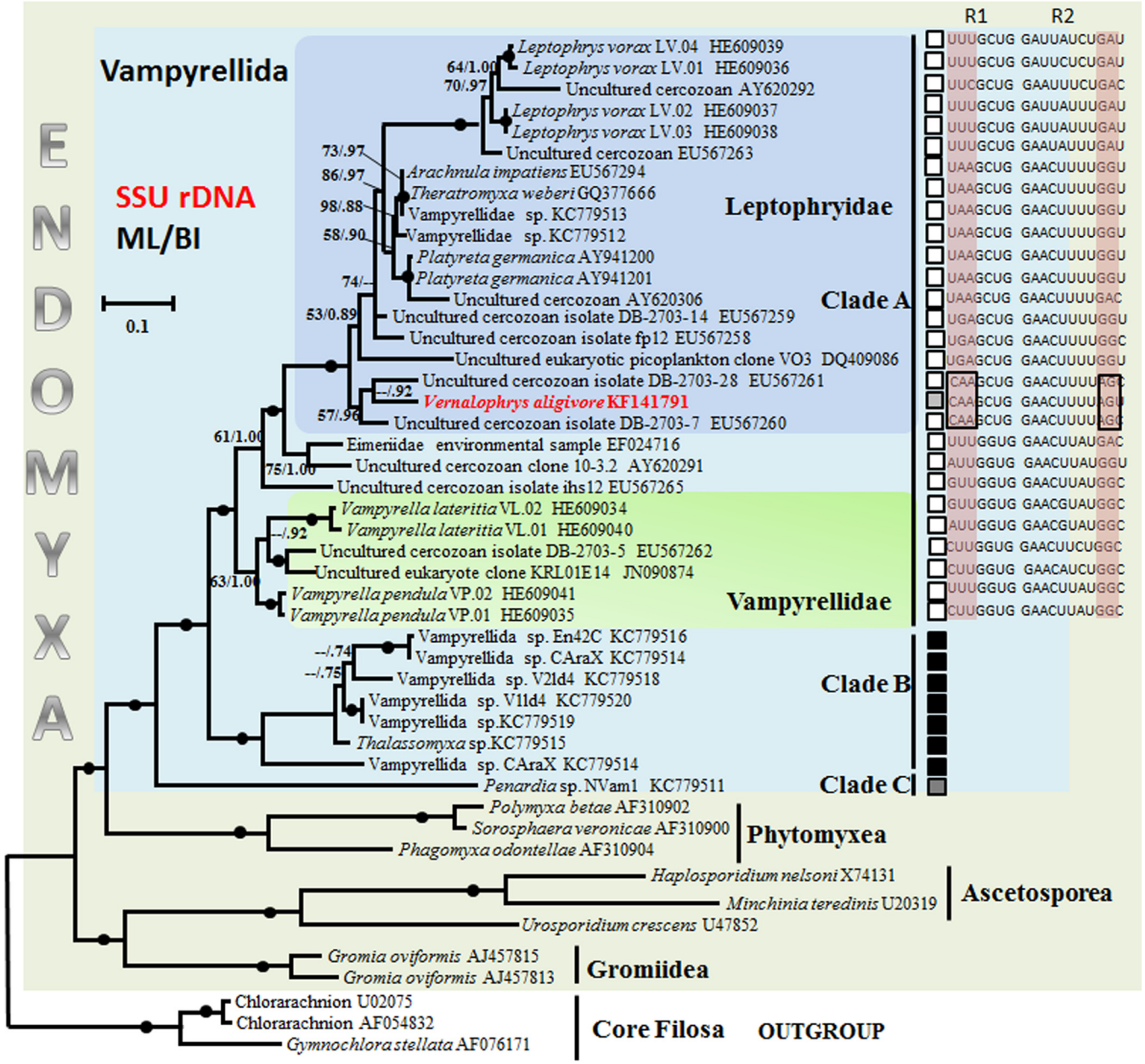

FIG 8 SSU rDNA phylogeny of vampyrellids, showing the position of *V. algivore* with other published vampyrellid isolates and related environmental clones from GenBank. Three chlorarachniophytes were used to root the tree. This is the maximum-likelihood tree obtained by PhyML analyses (34) of 47 sequences using 2,148 aligned characters. Bootstrap support values after 1,000 replicates and Bayesian posterior probabilities are indicated at nodes when they are above 50% and 0.70, respectively. The black circles represent support values at or above 90%/0.95. Vampyrellids cluster in three main clades, A, B, and C. The black squares identify marine sequences, the white squares identify terrestrial (soil or freshwater) sequences, and the gray squares identify the species from brackish sediments. The aligned SSU rRNA sequences represent regions of helix E10_1 and E23_1. R1 and R2 represent partial sequences of E10_1 (nucleotides 117 to 123) and E23_1 (nucleotides 514 to 524), respectively, in the aligned SSU rRNA gene sequences; the nucleotide positions were based on the SSU rRNA gene sequence of *Leptophrys vorax* LV.03 (HE609038). Scale bar = 0.1, indicating that the sequence divergence is 10%.

with *Leptophrys* in the molecular phylogenetic tree (Fig. 8). As for the genus *Arachnula*, the digestive cyst and resting cyst stages have long, tapering, empty spines that are not found in other vampyrellids (43), including our species. Members of the genus *Platyreta* can form zoospores with two flagella (45), a feature not reported in any other vampyrellids and not observed in *Vernalophrys*. Finally, the genus *Theratromyxa* feeds on nematodes, which makes it quite different from *Vernalophrys* and other leptophryids. In addition to the above-mentioned differences, some features of *V. algivore* have not yet been observed in other vampyrellids. They include (i) preference for *Scenedesmus* as food, which has not previously been reported as a food source for vampyrellids; (ii) trophozoites and cysts aggregate to form flocs (Fig. 6E); (iii) two distinctive regions in helix E10_1 (Fig. 8) (nucleotides 117 to 119; CAA) and E23_1 (Fig. 8) (nucleotides 522 to 523; AG).

These characteristics, along with the molecular phylogenetic anal-

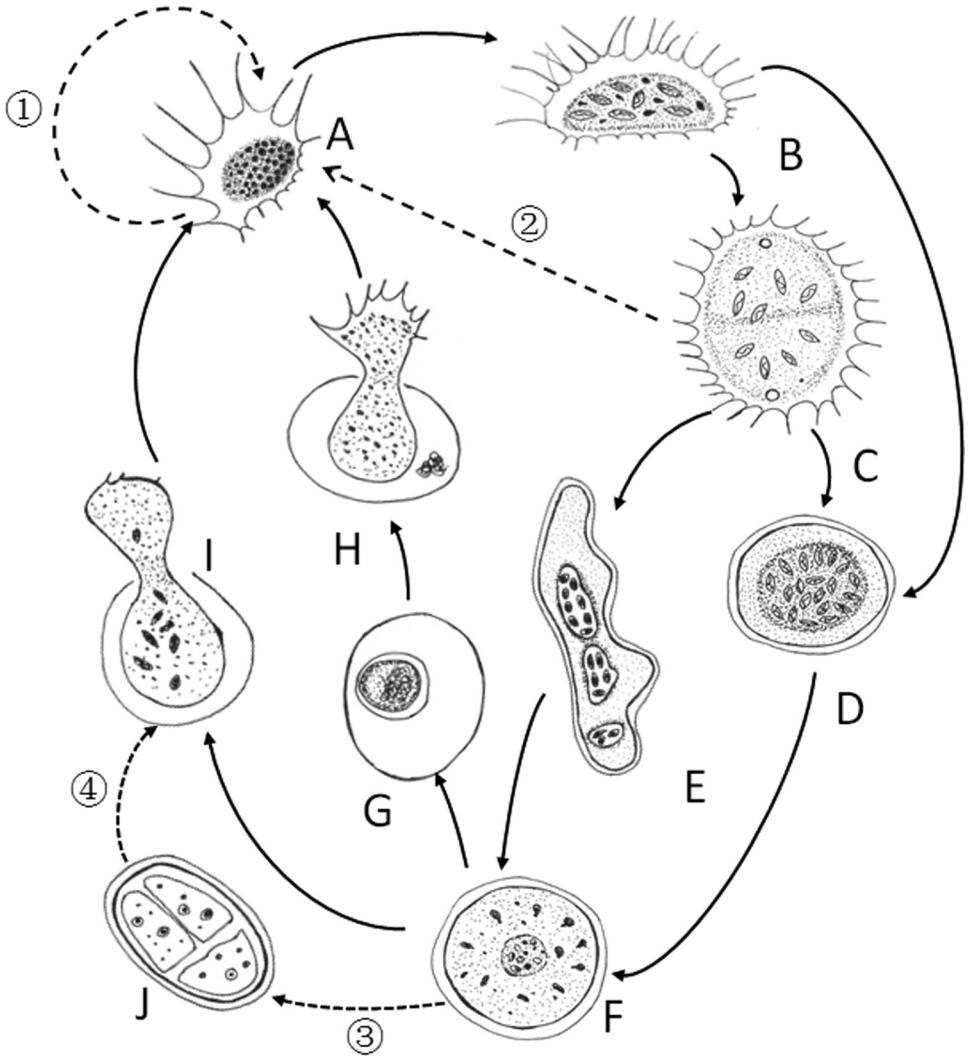

FIG 9 Diagram showing transformations in gross morphology in the possible life cycle of *V. algivore*. (A) Trophozoite. (B) Trophozoite with ingested algal cells. (C) Plasmodia formed by fusion of two trophozoites. (D) Round digestive cyst in an early stage. (E) Irregularly shaped digestive cyst transformed from plasmodium. (F) Digestive cyst in a late stage. (G) Resting cyst. (H) Excystment of a young trophozoite from the resting cyst. (I) Excystment of young trophozoites from the digestive cyst. (J) Cell division inside the cyst. The solid arrows indicated that the transformations were observed in this study, while the dashed arrows indicate that the transformations were not observed in our study but probably existed. As is shown, cell division may take place in the trophozoite stage (A, 1), the plasmodium stage (C, 2), or the digestive cyst stage (J, 3 and 4) or during excystation (I). Due to the dense matrix of the central cytoplasm, it was not usually possible to observe the distinct organelles, such as nuclei and contractile vacuoles.

ysis (Fig. 8), distinguish *Vernalophrys* from all existing vampyrellids. The phylogenetic analysis, including previously published isolates and identified environmental clones from GenBank, places *V. algivore* at the base of clade A. It did not group with any known genus but clustered with two freshwater environmental colonies sharing two unique sequence regions with *V. algivore* (Fig. 8). This supports the establishment of the new genus *Vernalophrys*, in which *V. algivore* is the only species. The species name "*algivore*" emphasizes that the amoeba feeds on algae. Based upon our limited experiments, we know that the amoeba does not feed on *C. zofingiensis* and *N. oceanica*, but we do not know if the amoeba feeds on other microalgae.

Distribution and environmental considerations. As predators of algae, fungi, protozoa, and small metazoa, vampyrellids are common in soils, freshwater and marine water columns, and sediments and are suspected to have a significant role in microbial ecosystems (24, 46). However, little is known about their distribution in large-scale algal cultures in which plenty of prey algae are available. This study is the first report of a vampyrellid from a mass culture of *S. dimorphus*. Its impact on *S. dimorphus* is rapid and devastating, causing a population crash (47) that can reduce algal cell density and biomass productivity to 1/5 to 1/10 those of controls (Fig. 1). This prevents the development of commercial mass cultures of *S. dimorphus*.

As *V. algivore* did not occur in indoor cultures and was not present in outdoor cultures with smaller volumes, we concluded that it arrived in the outdoor raceway ponds and closed photobioreactors as a contaminant from the environment but not from the seed culture. This conclusion is also supported by the phylogenetic tree (Fig. 8), in which *V. algivore* has close relationships with

Arachnula (45), *Platyreta* (45), and *Theratromyxa* (20), all of which can occur in soils. It is possible that *V. algivore* can live in soils, perhaps as cysts, and may be transported to an algal culture by air or animal movements.

Our phylogenetic results were consistent with the previous analysis (14) that the soil dwellers (the Leptophryidae, such as *Platyreta*, *Theratromyxa*, and *A. impatiens*) likely emerged from limnetic ancestors (the Vampyrellidae, such as *Vampyrella*) that are located closer to the base of the clade (Fig. 8).

As Berney et al. (24) mentioned, some strains of vampyrellids were difficult to maintain in culture even when a suitable food source was apparently available. *V. algivore* did not thrive with *S. dimorphus* as food under laboratory conditions. This is a challenge that must be addressed if we wish to develop methods that prevent the outbreak of the amoebae in outdoor algal cultures.

Special feeding characteristics of the vampyrellid on algae. The first report of vampyrellids feeding on algae by Cienkowski in 1865 (16) referred to their capacity to perforate algal cell walls and extract the algal cytoplasm. Now, 150 years later, seven genera, including over 30 species from soil and freshwater, have been reported, and most prey on algae by engulfment or penetration (14, 15, 20, 22, 44, 45) (see Table S5 in the supplemental material). The prey algae of vampyrellids include unicellular or filamentous green algae, such as *Closterium*, *Oedogonium*, *Zygnema*, and *Ulothrix*, and some diatoms, such as *Gloserium* (14, 15, 20) (see Table S5 in the supplemental material), as well as fungi (by penetration) (21, 23) and nematodes (by engulfment) (22). Berney et al. (24) recently showed that vampyrellids are much more diverse than previously thought.

In this study, we reported one new species, *V. algivore*, from mass culture of *Scenedesmus*. We have convincing data (see Movie S2 in the supplemental material) to show how the amoeba attacks *Scenedesmus* cells by engulfment. However, the light and scanning electron microscopic observations suggest that the digestive cyst may be able to attach to algal cells and even suck the cytoplasm of the algal cells (Fig. 3J and 6C).

Considering their aggressive algivorous characters, vampyrellids deserve more attention as potential threats to commercial algal cultures.

ACKNOWLEDGMENTS

This project was partially supported by U.S. Agriculture and Food Research Initiative Competitive Grant no. 2011-67009-30112 from the USDA National Institute of Food and Agriculture and the State Development and Investment Corporation in China.

We are indebted to Michael Melkonian and Sebastian Hess from the University of Cologne (Germany) for their valuable advice and critical review of the manuscript. We also thank Steven W. Van Ginkel from the Georgia Institute of Technology (USA) for helpful advice on the manuscript.

REFERENCES

1. **Hintz HF, Heitman H, Weir WC, Torell DT, Meyer JH.** 1966. Nutritive value of algae grown on sewage. J Anim Sci **25:**675–681.
2. **Qin S, Liu GX, Hu ZY.** 2008. The accumulation and metabolism of astaxanthin in *Scenedesmus obliquus* (Chlorophyceae). Process Biochem **43:**795–802. http://dx.doi.org/10.1016/j.procbio.2008.03.010.
3. **Wiltshire KH, Boersma M, Möller A, Buhtz H.** 2000. Extraction of pigments and fatty acids from the green alga *Scenedesmus obliquus* (Chlorophyceae). Aquat Ecol **34:**119–126. http://dx.doi.org/10.1023/A:1009911418606.
4. **Mandal S, Mallick N.** 2009. Microalga *Scenedesmus obliquus* as a potential source for biodiesel production. Appl Microbiol Biotechnol **84:**281–291. http://dx.doi.org/10.1007/s00253-009-1935-6.
5. **Carney LT, Lane TW.** 2014. Parasites in algae mass culture. Front Microbiol **5:**278. http://dx.doi.org/10.3389/fmicb.2014.00278.
6. **Soeder CJ, Maiweg D.** 1969. Einfluss pilzlicher Parasiten auf unsterile Massenkulturen von *Scenedesmus*. Arch Hydrobiol **66:**48–55.
7. **Letcher PM, Lopez S, Schmieder R, Lee PA, Behnke C, Powell MJ, McBride RC.** 2013. Characterization of *Amoeboaphelidium protococcarum*, an algal parasite new to the Cryptomycota isolated from an outdoor algal pond used for the production of biofuel. PLoS One **8:**e56232. http://dx.doi.org/10.1371/journal.pone.0056232.
8. **Schnepf E, Hegewald E, Soeder CJ.** 1974. Elektronenmikroskopische Beobachtungen an Parasiten aus Scenedesmus. Massenkulturen 4. Bakterien Arch Microbiol **98:**133–145.
9. **Abeliovich A, Dikbuck S.** 1977. Factors affecting infection of *Scenedesmus obliquus* by a *Chytridium* sp. in sewage oxidation ponds. Appl Environ Microbiol **34:**832–836.
10. **Gromov BV, Mamkaeva KA.** 1969. Sensitivity of different *Scenedesmus* strains to the endoparasitic microorganism *Amoeboaphelidium*. Phycologia **7:**19–23.
11. **Pinevich A, Gromov B, Mamkaeva K, Nasonova E.** 1997. Study of molecular karyotypes in *Amoeboaphelidium protococcarum*, the endotrophic parasite of Chlorophycean alga *Scenedesmus*. Curr Microbiol **34:**122–126. http://dx.doi.org/10.1007/s002849900155.
12. **Huessler P, Castillo SJ, Merino MF.** 1978. Parasite problems in the outdoor cultivation of *Scenedesmus*. Arch Hydrobiol Beih Erg Limnol **11:**223–227.
13. **Karpov SA, Mamkaeva MA, Aleoshin VV, Nassonova E, Osu L, Gleason FH.** 2014. Morphology, phylogeny, and ecology of the aphelids (Aphelidea, Opisthokonta) and proposal for the new superphylum Opisthosporidia. Front Microbiol **5:**112. http://dx.doi.org/10.3389/fmicb.2014.00112.
14. **Hess S, Sausen N, Melkonian M.** 2012. Shedding light on vampires: the phylogeny of vampyrellid amoebae revisited. PLoS One **7:**e31165. http://dx.doi.org/10.1371/journal.pone.0031165.
15. **Röpstorf P, Hülsmann N, Hausmann K.** 1994. Comparative fine structural investigations of interphase and mitotic nuclei of vampyrellid filose amoebae. J Eukaryot Microbiol **41:**18–30. http://dx.doi.org/10.1111/j.1550-7408.1994.tb05930.x.
16. **Cienkowski L.** 1865. Beiträge zur Kenntnis der Monaden. Arch Mikrosk Anat **5:**203–232.
17. **Cienkowski L.** 1876. Über einige Rhizopoden und verwandte Organismen. Arch Mikrosk Anat **12:**15–50.
18. **Zopf W.** 1885. Die Pilzthiere oder Schleimpilze, p 1–174. *In* Schenk A (ed), Handbuch der Botanik (Encykl. Naturwiss.). Trewendt, Breslau, Germany.
19. **Lloyd FE.** 1926. Some features of structure and behaviour in *Vampyrella lateritia*. Science **63:**364–365. http://dx.doi.org/10.1126/science.63.1631.364.
20. **Hülsmann N.** 1993. *Lateromyxa gallica* n. g., n. sp. (Vampyrellidae): a filopodial amoeboid protist with a novel life cycle and conspicuous ultrastructural characters. J Eukaryot Microbiol **40:**141–149. http://dx.doi.org/10.1111/j.1550-7408.1993.tb04894.x.
21. **Old KM, Darbyshire JF.** 1980. *Arachnula impatiens* Cienk, a mycophagous giant amoeba from soil. Protistologica **16:**277–287.
22. **Sayre RM.** 1973. *Theratromyxa weberi*, an amoeba predatory on plant-parasitic nematodes. J Nematol **5:**258–264.
23. **Old KM, Chakraborty S.** 1986. Mycophagous soil amoebae: their biology and significance in the ecology of soil-borne plant pathogens. Prog Protistol **1:**163–194.
24. **Berney C, Romac S, Mahé F, Santini S, Siano R, David B.** 2013. Vampires in the oceans: predatory cercozoan amoebae in marine habitats. ISME J **7:**2387–2399. http://dx.doi.org/10.1038/ismej.2013.116.
25. **Allen MM, Stanier RY.** 1968. Growth and division of some unicellular blue-green algae. J Gen Microbiol **51:**199–202. http://dx.doi.org/10.1099/00221287-51-2-199.
26. **Rippka R, Deruelles J, Waterbury JB, Herdman M, Stanier RY.** 1979. Generic assignments, strain histories and properties of pure cultures of cyanobacteria. J Gen Microbiol **111:**1–61. http://dx.doi.org/10.1099/00221287-111-1-1.
27. **Hanaichi T, Sato T, Iwamoto T, Malavasi-Yamashiro J, Hoshino M, Mizuno N.** 1986. A stable lead by modification of Sato's method. J Electron Microsc (Tokyo) **35:**304–306.
28. **Gong YC, Yu YH, Villalobo E, Zhu FY, Miao W.** 2006. Reevaluation of the phylogenetic relationship between mobilid and sessilid peritrichs (Ciliophora, Oligohymenophorea) based on small subunit rRNA gene se-

quences. J Eukaryot Microbiol **53:**397–403. http://dx.doi.org/10.1111/j.1550-7408.2006.00121.x.
29. **Medlin L, Elwood HJ, Stickel S, Sogin ML.** 1998. The characterization of enzymatically amplified eukaryotic 16S7 like rRNA7 coding regions. Gene **71:**4917499.
30. **Fokam Z, Ngassam P, Strüder Kypke MC, Lynn DH.** 2011. Genetic diversity and phylogenetic position of the subclass *Astomatia* (Ciliophora) based on a sampling of six genera from West African oligochaetes (Glossoscolecidae, Megascolecidae), including description of the new genus *Paraclausilocola* n. gen. Eur J Protistol **47:**161–171. http://dx.doi.org/10.1016/j.ejop.2011.02.002.
31. **Thompson JD, Gibson TJ, Plewniak F, Jeanmougin F, Higgins DG.** 1997. The Clustal X windows interface: flexible strategies for multiple sequence alignment aided by quality analysis tools. Nucleic Acids Res **25:**4876–4882. http://dx.doi.org/10.1093/nar/25.24.4876.
32. **Gouy M, Guindon S, Gascuel O.** 2010. SeaView version 4: a multiplatform graphical user interface for sequence alignment and phylogenetic tree building. Mol Biol Evol **27:**221–224. http://dx.doi.org/10.1093/molbev/msp259.
33. **Tamura K, Stecher G, Peterson D, Filipski A, Kumar S.** 2013. MEGA6: molecular evolutionary genetics analysis version 6.0. Mol Biol Evol **30:**2725–2729. http://dx.doi.org/10.1093/molbev/mst197.
34. **Guindon S, Dufayard JF, Lefort V, Anisimova M, Hordijk W, Gascuel O.** 2010. New algorithms and methods to estimate maximum-likelihood phylogenies: assessing the performance of PhyML 3.0. Syst Biol **59:**307–321. http://dx.doi.org/10.1093/sysbio/syq010.
35. **Farris JS.** 1970. Methods for computing Wagner trees. Syst Zool **19:**83–92. http://dx.doi.org/10.2307/2412028.
36. **Saitou N, Nei M.** 1987. The neighbor-joining method: a new method for reconstructing phylogenetic trees. Mol Biol Evol **4:**406–425.
37. **Huelsenbeck JP, Ronquist F.** 2001. MrBayes: Bayesian inference of phylogeny. Bioinformatics **17:**754–755. http://dx.doi.org/10.1093/bioinformatics/17.8.754.
38. **Posada D, Crandall KA.** 1998. Model test: testing the model of DNA substitution. Bioinformatics **14:**817–818. http://dx.doi.org/10.1093/bioinformatics/14.9.817.
39. **Swofford DL.** 2002. PAUP*. Phylogenetic analysis using parsimony (*and other methods), version 4. Sinauer Associates, Sunderland, MA.
40. **Rannala B, Yang Z.** 1996. Probability distribution of molecular evolutionary trees: a new method of phylogenetic inference. J Mol Evol **43:**304–311. http://dx.doi.org/10.1007/BF02338839.
41. **Heinbokel JF.** 1978. Studies on the functional role of tintinnids in the Southern California Bight. I. Grazing and growth rates in laboratory cultures. Mar Biol **47:**177–189.
42. **Patterson DJ, Surek B, Melkonian M.** 1987. The ultrastructure of *Vampyrellidium perforans* Surek & Melkonian and its taxonomic position among the naked filose amoebae. J Protozool **34:**63–67. http://dx.doi.org/10.1111/j.1550-7408.1987.tb03133.x.
43. **Canter HM.** 1973. A new primitive protozoan devouring centric diatoms in the plankton. Zool J Limnol Soc **52:**63–83. http://dx.doi.org/10.1111/j.1096-3642.1973.tb01878.x.
44. **Surek B, Melkonian M.** 1980. The filose amoeba *Vampyrellidium perforans* nov. sp. (Vampyrellidae, Aconchulinida): axenic culture, feeding behaviour and host range specificity. Arch Protistenkd **123:**166–191. http://dx.doi.org/10.1016/S0003-9365(80)80003-0.
45. **Bass D, Chao EEY, Nikolaev S, Yabuki A, Ishida K, Berney C, Pakzad U, Wylezich C, Cavalier-Smith T.** 2009. Phylogeny of novel naked filose and reticulose cercozoa: Granofilosea cl. n. and Proteomyxidea revised. Protist **160:**75–109. http://dx.doi.org/10.1016/j.protis.2008.07.002.
46. **Bonkowski M, Cheng W, Griffiths BS, Alphei J, Scheu S.** 2000. Microbial faunal interactions in the rhizosphere and effects on plant growth. Eur J Soil Biol **36:**135–147. http://dx.doi.org/10.1016/S1164-5563(00)01059-1.
47. **Rockwood LL.** 2006. Introduction to population ecology. Blackwell, Malden, MA.